

Evaluation of physicochemical characteristics of hydrophobically modified glycol chitosan nanoparticles and their biocompatibility in murine osteosarcoma and osteoblast-like cells

Amanda Chin¹, Giulia Suarato¹, Yizhi Meng^{1,2*}

¹Department of Materials Science & Engineering, Stony Brook University, New York, USA

²Program of Chemical & Molecular Engineering, Stony Brook University, New York, USA

*Corresponding author: Yizhi Meng, Department of Materials Science & Engineering, Stony Brook University, New York, USA; Tel: 631 632 8552; Fax: 631 632 8052; E-mail: yizhi.meng@stonybrook.edu

Received Date: January 02, 2014 Accepted Date: January 14, 2014 Published Date: January 31, 2014

Citation: Yizhi Meng (2014) Evaluation of physicochemical characteristics of hydrophobically modified glycol chitosan nanoparticles and their biocompatibility in murine osteosarcoma and osteoblast-like cells. J Nanotech Smart Mater 1: 1-7

Abstract

Glycol chitosan, a derivative of chitosan, can be hydrophobically modified by 5 β -cholanolic acid to impart amphiphilic properties that enable the self-assembly into nanoparticles in aqueous media at neutral pH. This nanoparticle system has shown initial success as a therapeutic agent in several model cell culture systems, but little is known about its stability against enzymatic degradation. The goal of this research was therefore to investigate the physicochemical properties of hydrophobically modified glycol chitosan nanoparticles (CNP) under exposure to lysozyme, a ubiquitous mammalian enzyme. Dynamic light scattering (DLS) revealed that the CNP vehicles had an average hydrodynamic diameter of 288.6 nm. These nanoparticles were able to encapsulate bovine serum albumin (BSA) at 87-90% efficiency. Varying the initial CNP: BSA mass ratio affected both particle size and total protein release, indicating a difference in complexation between the negatively charged protein and the positively charged chitosan polymer when more cargo is loaded. After 3 hours of exposure to lysozyme, CNP vehicles degraded to 10-150 nm particles, whereas BSA-loaded CNP degraded more extensively to predominantly 10-20 nm particles. Interesting, however, the encapsulated BSA was not fragmented as shown by SDS-PAGE. Minimal cytotoxicity of the CNP vehicles was observed in both rat osteosarcoma (ROS 17/2.8) and murine osteoblast-like (MC3T3-E1) cells, which internalized the nanoparticles within 2 hours. Taken together, these data suggest that hydrophobically modified glycol chitosan nanoparticles are a promising smart material for use in controlled release drug delivery systems.

Keywords: Drug delivery, Glycol Chitosan Nanoparticles, Self-assembled

Introduction

The success of cancer drug delivery systems largely depends on their ability to accumulate in the target tissues with minimal loss while in the blood circulation, and the controlled release of the therapeutic inside the tumor cells [1, 2]. For example, reducing the size of the vehicles from micro- to nano-sized (100-200 nm) can slow down the rapid clearance from the circulation by macrophages of the reticuloendothelial system (RES) following intravenous administration [3]. To achieve targeted delivery, various delivery systems have utilized the tumor-homing characteristic of nanocarriers [4, 5]. This passive strategy exploits the enhanced permeability and retention

(EPR) of the tumor microenvironment due to its rapid growth that prevents the formation of fully functional vasculature and proper lymphatic drainage [1, 2, 6]. To promote site-specific targeted release of therapeutics, one strategy is to design stimuli responsive micelles that are very sensitive to intracellular pH [7] and enzymatic activity [8]. Often this increases the anticancer efficacy of the payload, thus reducing the therapeutic dose and the possibility of side effects [9].

Chitosan has emerged as a prominent nanomaterial for biomedical applications due to its biocompatibility, biodegradability, abundant availability, and low cost [10-12]. Native chitosan has poor water solubility at physiological pH and is limited in its biomedical application [13, 14]. This can be improved by chemical modification, such as by introducing a hydrophobic or a hydrophilic moiety [15], an alkyl group [16], cholesterol [17], or poly(ethylene glycol) (PEG) [18-24].

©2013 The Authors. Published by the JScholar under the terms of the Creative Commons Attribution License <http://creativecommons.org/licenses/by/3.0/>, which permits unrestricted use, provided the original author and source are credited.

Recently, hydrophobic modification of glycol chitosan, a derivative of chitosan, has been shown to assist in the formation of stable amphiphilic nanocomplexes that are capable of entrapping both hydrophilic peptides [25] and low water soluble drugs [4, 26-30]. These nanoparticles were successfully used to demonstrate selective accumulation in tumors of mice using a near-infrared fluorescent (NIRF) label [31].

Physiological enzymes can rapidly depreciate system drug circulation, and therefore the *in vivo* stability of chitosan-based drug carriers is an important criterion for predicting their therapeutic efficacy. Elevated serum levels of lysozyme, a universal mammalian enzyme, have been observed in tumor-bearing rats as well as patients with solid tumors [32]. Because lysozyme breaks down the sugar linkages of polysaccharide chains by hydrolysis, it may also degrade chitosan-based carriers [10, 33]. However, the effect of lysozyme on these nanoparticles and their payload is not well known and is the focus of this study.

Materials and methods

Materials

Glycol chitosan (250 kDa molecular weight, degree of deacetylation >60%), 5 β -cholic acid, N-(3-dimethylaminopropyl)-N'-ethylcarbodiimide hydrochloride (EDC), N-hydroxysuccinimide (NHS), lysozyme from chicken egg white, and bicinonic acid (BCA) assay were purchased from Sigma-Aldrich (St. Louis, MO). Monoreactive hydroxysuccinimide ester of Cyanine 5.5 (Cy5.5-NHS) was obtained from Lumiprobe (Hallandale Beach, FL). Anhydrous dimethyl sulfoxide (DMSO) and bovine serum albumin (BSA) were purchased from EMD Chemicals Inc. (Darmstadt, Germany). Analytical grade methanol was acquired from Pharmco-AAPER (Brookfield, CT). Rat osteosarcoma (ROS) 17/2.8 cells were kindly provided by Professor Miriam Rafailovich and subclone 4 mouse calvaria-derived (MC3T3-E1) cells were obtained from ATCC (Manassas, VA). Fluoromount-G was purchased from Southern Biotech (Birmingham, AL).

Synthesis of 5 β -cholic acid-conjugated glycol chitosan nanoparticles

Water-soluble glycol chitosan (500 mg) was first dissolved in deionized (DI) water (60 mL). The carboxylic acids groups of 5 β -cholic acid were then activated with 1.5 equivalents of N-hydroxysuccinimide (NHS) and N-(3-Dimethylaminopropyl)-N'-ethylcarbodiimide hydrochloride (EDC) dissolved in methanol (60 mL). The hydrophobic modification of glycol chitosan was carried out by slowly combining to two solutions under stirring for 24 hours at room temperature to permit the 5 β -cholic acid to conjugate to the chitosan through the formation of amide linkages. The solution was dialyzed in a dialysis membrane (10 kDa molecular weight cut off) for 24 hours against a water/methanol mixture (1:4 v/v) and the following 24 hours against DI water. The purified solution was lyophilized and ground into a fine powder. The conjugates were suspended in either DI water or phosphate-buffered saline (PBS) at a concentration of 1 mg/mL and probe-type sonicated (S-450D Sonifier, Branson Ultrasonics,

Danbury, CT) at 90 W for two minutes. This sonication step was repeated three times to ensure that the self-assembly of the conjugates into nanoparticles.

Cy5.5- labeling of chitosan nanoparticles

Cy5.5 is one of the most prominent near infrared dyes which can be used for noninvasive imaging of live animals, but to some extent its usage is restricted by insufficient hydrophilicity [34]. To fluorescently label the hydrophobically modified glycol chitosan, Cy5.5-NHS (1 mg) was first dissolved in dimethyl sulfoxide (DMSO, 250 μ L) and subsequently added dropwise to a bulk solution of 5 β -cholic acid-conjugated glycol chitosan. The resulting vividly blue solution was then stirred for 6 hours at room temperature, shielded from light. The Cy5.5-labeled conjugate solution was then dialyzed (10 kDa molecular weight cut off) in DI water to remove unreacted Cy5.5 molecules. Following 2 days of dialysis, the solution was lyophilized and ground to produce a blue powder. In order to protect the fluorescent properties of the Cy5.5 dye, these processes were performed in the dark. The Cy5.5-labeled conjugates were then probe-type sonicated as described above to form self-assembled fluorescent nanoparticles. Prior to cell culture, the nanoparticle solutions were passed through a 0.2 μ m syringe filter to remove aggregates and biological contaminants.

Characterization of chitosan nanoparticles

The size and zeta potential of the chitosan nanoparticles (CNP) were measured at 25°C using dynamic light scattering (DLS) with a 633 nm laser (Malvern Zetasizer Nano – ZS; Malvern, Worcestershire, UK). The zeta potential is the measure of surface charge of nanoparticles and is a particularly influential parameter to understand the electrostatic interaction between nanoparticles. This characteristic is also suggestive of a nanoparticle's affinity to penetrate negatively charged biological membranes. CNP suspensions prepared in water at a concentration of 1 mg/mL were further sonicated in a water bath for 10 minutes at room temperature prior to DLS measurements. Additionally, a separate bath of CNP suspension was stored in water at 4°C and particle size was measured using the DLS over the course of 10 days to determine the size stability. Average values were calculated from a minimum of three measurements. Standard error was calculated by dividing the standard deviation by the square root of n, the sample size.

Protein encapsulation and release kinetics

The model protein, bovine serum albumin (BSA), was used to evaluate the encapsulation efficiency of the hydrophobically modified glycol chitosan nanoparticles (CNP). Separate solutions of BSA and chitosan conjugates were first prepared in PBS. Two CNP:BSA mass loading ratios were used: 10:1 and 10:2. Immediately after combining, the BSA and chitosan mixture was probe-type sonicated to form self-assembled nanoparticles. Triplicates of each sample were prepared and analyzed.

To calculate the loading efficiency of BSA, each BSA-CNP solution was first centrifuged at 3,000 RPM for 30 min and the supernatant was separated from the pellet. The concentration of BSA in the supernatant, which represented the total amount

of protein that was not loaded into the nanoparticles, was determined using a bicinchoninic acid assay (BCA assay) (Quantipro™, Sigma-Aldrich). Absorbance at 562 nm was measured with a Microplate reader (ELx800, BIO-TEK, Winooski, VT). The loading efficiency was calculated using the following equation:

$$\text{loading efficiency (\%)} = \frac{\text{mass of total BSA used} - \text{mass of BSA remaining in supernatant}}{\text{mass of total BSA used}} \times 100$$

Enzymatic degradation

Because lysozyme levels throughout the body range in concentration from 0.8 mg/mL to 1.7 mg/mL [35, 36], we decided to examine the degradation of CNPs at the highest level and prepared a 1.7 mg/mL solution (pH 7.2) from a 10 mg/mL stock solution. A lysozyme inactivation solution was prepared containing 4% sodium dodecyl sulfate (SDS), 1 M Tris-HCl (pH = 6.8), and 20% glycerol in DI water. Lysozyme solution was added to suspensions of CNPs to a final volume of 3 mL, and the mixture was incubated for 3 hours at 37°C in a rotating incubating shaker at 55 RPM (Excelsa E24, New Brunswick Scientific, Enfield, CT). Particle size was measured with DLS after 0 min, 30 min, 60 min, 120 min, 150 min, and 180 min of incubation at room temperature. A 0.5 mL aliquot of each sample was harvested at each time point and placed in an eppendorf tube with 0.5 mL of inactivation solution prior to being centrifuged at 10,000 g for 10 min. The supernatants were then collected for analysis in the DLS. The total volume of each sample was kept at 3 mL between time points to maintain sink conditions.

Transmission electron microscopy (TEM)

CNP vehicles (1 mg/mL) and BSA-CNPs prepared at both 10:1 and 10:2 mass loading ratios were incubated with either water or lysozyme (1.7 mg/mL) for 3 hours and immediately deposited onto 300-mesh copper TEM grids coated with a Lacey film. The air dried grids were imaged on a JEOL 1400 TEM (Peabody, MA) at an accelerating voltage of 60 keV.

Sodium dodecyl sulfate polyacrylamide gel electrophoresis (SDS-PAGE)

Sodium dodecyl sulfate polyacrylamide gel electrophoresis (SDS-PAGE) was used to evaluate the integrity of BSA-loaded CNPs after exposure to either water or lysozyme. BSA loading at both 10:2 and 10:1 were evaluated. Samples were loaded into 10% pre-cast acrylamide gels and run under a constant voltage of 90 V.

Cell culture

Rat osteosarcoma (ROS 17/2.8) and mouse calvaria-derived (MC3T3-E1) cell lines were maintained in α -modified minimum essential medium (α -MEM) supplemented with 10% fetal bovine serum (FBS) and 1% penicillin streptomycin (Pen-Strep) at 37°C with a humidified 5% CO₂ atmosphere. The cells were seeded onto glass coverslips (12 mm diameter, #1) in 24-well tissue culture plates (Becton Dickinson, Franklin Lakes, NJ) at a density of 10,000 cells/cm² and medium was refreshed every two days. After attaching for 24 hours, the

cells were rinsed twice with serum-free α -MEM to remove any remnants of FBS, and incubated for 2 hours with serum-free α -MEM containing CNPs at the following concentrations: 10 μ g/mL, 100 μ g/mL, and 1000 μ g/mL. The cells were then given fresh α -MEM supplemented with 10% FBS and 1% Pen-Strep and maintained at 37°C (5% CO₂, humidified) for up to 72 hours.

Cell viability

After 4 hr, 24 hr, 48 hr and 72 hr of incubation, the cells were fixed with 3.7% paraformaldehyde and rinsed two times with PBS before being fixing with 3.7% formaldehyde. Cells were rinsed two additional times with PBS and stained with the nuclear dye, 4',6-diamidino-2-phenylindole (DAPI). The area density of the cells was determined by enumerating DAPI-stained nuclei on an inverted fluorescence microscope (Olympus IX51). Cell viability was calculated as the number of cells in the treatment group divided by the number of cells in the untreated control group, which consisted of cells that were given only α -MEM (without nanoparticles).

In vitro delivery of protein-loaded Cy5.5-CNPs

BSA was first loaded into the Cy5.5-HGC conjugates at the mass loading ratio of 10:2 or 10:1 (CNP: BSA) by probe sonication. The final concentration of the BSA-loaded Cy5.5-CNP suspension was 1 mg/mL in α -MEM. After centrifugation at 4,000 RPM, the supernatant was aspirated to remove unbound BSA and the loaded nanoparticles were resuspended in serum-free α -MEM and filtered with both 0.8 μ m and 0.2 μ m syringe filters to remove aggregates and biological contaminants.

ROS 17/2.8 and MC3T3-E1 cells were seeded at a density of 10,000 cells/cm² into 24-well tissue culture plates (Becton Dickinson) containing glass coverslips. The cell lines were given α -MEM supplemented with 10% FBS and 1% Pen-Strep and were allowed to attach in 37°C incubator (5% CO₂, humidified) for 24 hours. The medium was then removed and the cells were rinsed with serum-free α -MEM. BSA-loaded Cy5.5-CNPs were then added to the medium so that the final concentration was 10 μ g/mL, 100 μ g/mL or 1000 μ g/mL. Cells were incubated with the nanoparticle solution for 2 hours.

Confocal laser scanning microscopy

Immediately after incubation in the CNP solution for 2 hours, the ROS and MC3T3-E1 cells were fixed with 3.7% formaldehyde, rinsed with PBS and stained with DAPI. The glass coverslips were mounted onto glass microscope slides using Fluoromount-G. Fluorescence images were captured on a confocal laser scanning microscope (Olympus IX81 Fluoview FV1000).

Results and Discussion

Chitosan:BSA massRatio	Average Diameter (nm)	Zeta Potential (mV)	Loading Efficiency (%)
10:0 (vehicle)	288.6 ± 21.8	13.2 ± 0.2	-
10:01	478.8 ± 9.6	12.7 ± 0.7	86.95 ± 2.90
10:02	374.8 ± 6.0	12.8 ± 0.4	89.91 ± 3.67

Table 1. Physicochemical parameters of hydrophobically modified glycol chitosan nanoparticles. Hydrodynamic diameter and zetal potential were measured in DI water. Loading efficiency of BSA encapsulation was measured in PBS.

Mean particle diameter of the chitosan nanoparticle (CNP) vehicles suspended in water at room temperature was 288.6 ± 21.8 nm (Table 1), respectively, similar to previously reported values [4, 31, 37]. The size of these nanoparticles was very stable and did not change significantly after 10 days of storage at 4°C (data not shown). Loading BSA onto the CNPs increased the average diameter of nanoparticles by 66% at the 10:1 CNP:BSA mass ratio (to 478.8 ± 9.6 nm) and by 30% at the 10:2 CNP:BSA mass ratio (to 374.8 ± 6.0 nm) (Table 1). The encapsulation efficiency was very similar at both BSA loading ratios, ranging from 87% to 90% (Table 1).

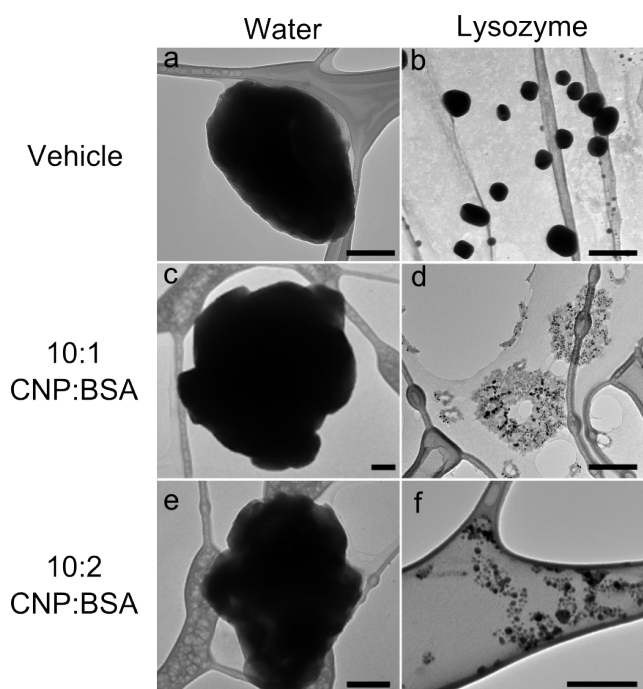


Figure 1. TEM images of CNP vehicles (a,b) and BSA-loaded CNP (c-f) in water (a,c,e) or 1.7 mg/mL lysozyme (b,d,f). Scale, 200 nm.

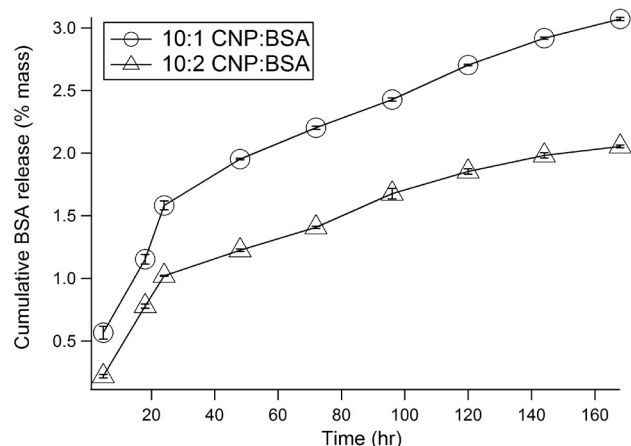


Figure 2. Release of bovine serum albumin (BSA) from chitosan nanoparticles suspended in PBS.

TEM images showed that both unloaded CNP vehicles and BSA-loaded CNPs suspended in water generally had a globular morphology, and that some of the nanoparticles also appeared to be aggregated (Fig. 1 c and e). These TEM images also confirmed that nanoparticles loaded with higher protein content (10:2 CNP:BSA mass ratio) were smaller in size than those loaded with lower protein content (10:1 CNP:BSA mass ratio). Previous studies have also reported a similar phenom-

enon when the RGD peptide was loaded into the same type of nanoparticles [25]. One possible explanation could be that in the case of higher protein content, there is an increase in electrostatic association between its negatively charged carboxylic and the positively charged amine groups on the chitosan backbone. As a result, chitosan is complexed to more strongly to the payload and the overall particle is more compact in size.

Average zeta potential of the CNP vehicles was 13.2 mV (Table 1), which is slightly lower than reported values for 359 nm nanoparticles [38]. The zeta potential of BSA-loaded CNPs was ~ 13 mV for both loading ratios (Table 1). Because of this similarity, we believe that the larger size of BSA-CNP resulted from the encapsulation of the BSA, and not from aggregation of protein on the outer surface of the nanoparticles.

Protein release from BSA-loaded CNP nanoparticles prepared at the two loading ratios showed an overall stable rate of release (up to only 3% after 7 days) (Fig. 2), indicating the existence of a strong complexation between BSA and chitosan. The rate of release did not vary greatly, as the slopes of both profiles are very similar. We also noticed that $\sim 50\%$ more protein was released from the 10:1 CNP:BSA nanoparticles (3.1%) than from the 10:2 CNP:BSA nanoparticles (2.1%) at the end of the 7-day period (Fig. 2). Taken together, these data suggest that the higher protein release observed for the larger nanoparticles was likely due to a looser packing of the protein at the lower loading ratio.

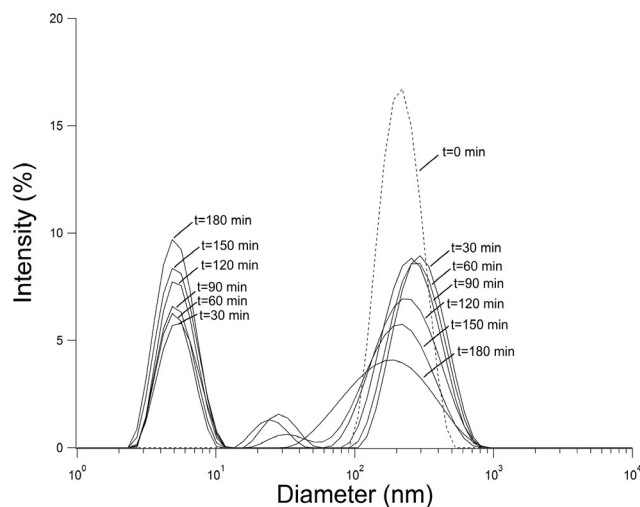


Figure 3. Size distribution of chitosan nanoparticles after exposure to lysozyme.

TEM images showed that exposure to lysozyme greatly reduced the size of the CNPs. After 3 hr, CNPs vehicles appeared as spherical moieties ranging from 10-150 nm in diameter (Fig. 1 b). This decrease in particle size is similar to previous reports on degradation of unmodified chitosan in the presence of lysozyme [39] and was expected, as lysozyme is known to hydrolyze the glycosidic linkages between consecutive sugar residues of chitosan [39]. BSA-loaded CNPs became transparent moieties in the presence of lysozyme and contained very small particles approximately 10-20 nm in size (Fig. 1 d,f).

Dynamic light scattering data showed a single peak in the range of 100 nm - 1000 nm for CNP vehicles exposed only to water ("t=0 min" in Fig. 3). This peak is in agreement with the TEM

images of the CNP vehicles suspended in water (Fig. 1a). As the nanoparticles underwent exposure to lysozyme, the height of this peak gradually decreased, suggesting that chitosan was being degraded. At the same time, a new peak in the range of 2 nm – 10 nm began to emerge, whose height and width both increased with incubation time, indicating an increase in the population of low molecular weight fragments. Another peak in the range of 10 nm – 50 nm also appeared, but its presence was not consistent and only appeared for samples incubated in lysozyme for 30 min, 60 min or 150 min.

Lane #	1	2	3	4	5	6	7	8	9
Chitosan nanoparticles	+	-	+	+	-	+	-	+	+
BSA (0.53 mg/mL)	-	+	+	-	-	-	+	+	-
BSA (0.28 mg/mL)	-	-	-	+	-	-	-	-	+
Lysozyme (1.7 mg/mL)	-	-	-	-	+	+	+	+	+

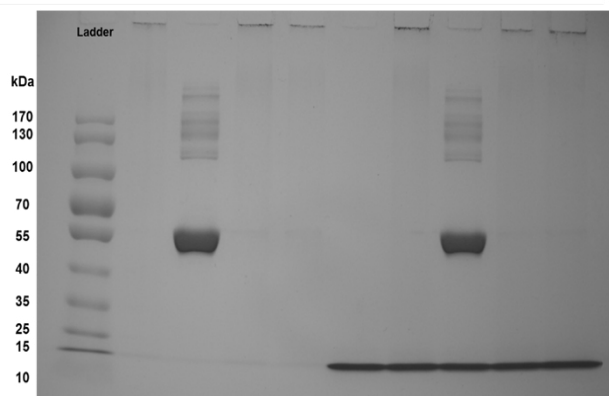


Figure 4. SDS-PAGE data of CNPs in water (lane 1), BSA in water (lane 2), BSA-CNP in water (lanes 3,4), lysozyme (lane 5), CNPs in lysozyme (lane 6), BSA in lysozyme (lane 7), and BSA-CNP in lysozyme (lanes 8,9).

SDS-PAGE data (Fig. 4) showed the sample remained in the well when it contained only chitosan (lanes 1,6), which was anticipated because only the negatively charged BSA was expected to migrate toward the positive electrode. Free BSA contained a very strong band around 55 kDa, as well as numerous high molecular weight fragments ranging in size from >170 kDa to 110 kDa (lane 2). When BSA was encapsulated in CNP, there was clearly an absence of fragments in the gel when either water (lanes 3-4) or lysozyme (lanes 8,9) was used as solvent, regardless of the CNP:BSA loading ratio. This indicated that encapsulated BSA was not easily degraded in both cases. When samples were incubated in lysozyme, a strong band appeared at ~15 kDa, which corresponded to the molecular weight of the enzyme (lanes 5-9).

Viability data of both osteosarcoma (ROS 17/2.8) and osteoblast-like (MC3T3-E1) cells showed that the CNP vehicles generally were not cytotoxic in the range of 0.01-1 mg/mL, as evidenced by the high cell viability (>90%) in both cell lines within the first 72 hours after exposure (Fig. 5). To ascertain cellular uptake of the nanoparticles, we collected fluorescence micrographs using a confocal laser scanning microscope and observed that Cy5.5-labeled CNP vehicles were successfully internalized by both the ROS and MC3T3-E1 cells within 2 hours (Fig. 6). The nanoparticles also appeared to be distributed more closely around the nucleus of the ROS cells (Fig. 6c) compared to the MC3T3-E1 cells, in which there was a more widespread accumulation of the nanoparticles throughout the cytoplasm (Fig. 6f).

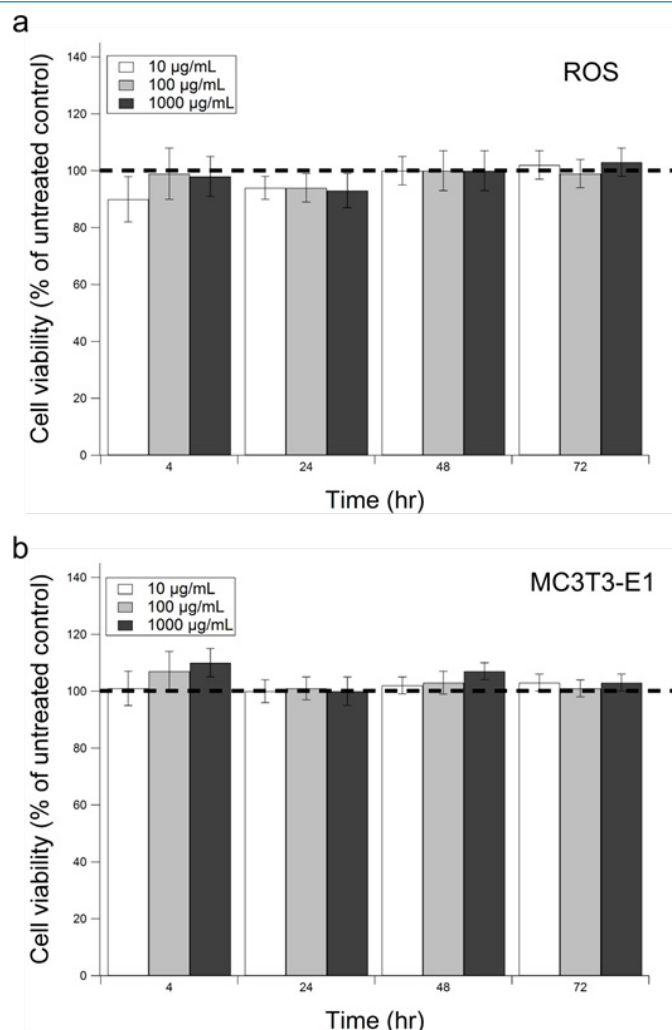


Figure 5. Viability of rat osteosarcoma (ROS) (a) and MC3T3-E1 (b) cells exposed to chitosan nanoparticles.

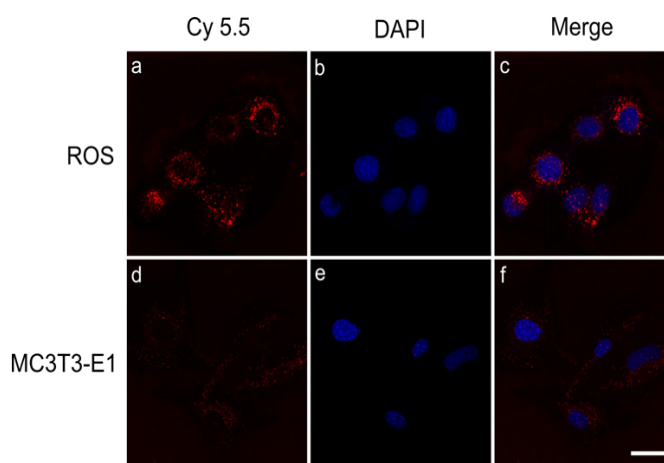


Figure 6. Confocal micrographs of ROS (a-c) and MC3T3-E1 (d-f) cells exposed to Cy5.5-CNPs (red channel). The nuclei of the cells are visualized in the blue channel. Scale, 20 µm.

Conclusions

Glycol chitosan was hydrophobically modified with 5β-cholanic acid and self-assembled into chitosan nanoparticles (CNPs) with an average hydrodynamic diameter of 288.6 nm. The CNPs were able to encapsulate bovine serum albumin (BSA) at 87-90% efficiency. Initially varying the CNP:BSA mass ratio

upon loading affected both particle size and total protein release, which indicates a difference in complexation between the negatively charged protein and the positively charged chitosan polymer. After 3 hours of exposure to lysozyme, CNP vehicles degraded to 10-150 nm particles, whereas BSA-loaded CNP degraded more extensively to 10-20 nm particles, however the encapsulated BSA was not fragmented. Minimal cytotoxicity of the CNP vehicles was observed in both rat osteosarcoma (ROS 17/2.8) and murine osteoblast-like (MC3T3-E1) cells, which internalized the nanoparticles within 2 hours. Taken together, these data suggest that hydrophobically modified glycol chitosan nanoparticles are a promising smart material for use in controlled release drug delivery systems.

Acknowledgments

We would like to thank the staff of the Center for Functional Nanomaterials, Brookhaven National Laboratory, especially Dr. Dmytro Nykypanchuk for his help with the DLS and zeta potential experiments. Research carried out in part at the Center for Functional Nanomaterials, Brookhaven National Laboratory, which is supported by the U.S. Department of Energy, Office of Basic Energy Sciences, under Contract No. DE-AC02-98CH10886.

References

- 1) K. Cho, X. Wang, S. Nie, Z. Chen, D.M. Shin (2008) Therapeutic nanoparticles for drug delivery in cancer, *Clinical Cancer Research*. 14: 1310-1316.
- 2) K. Greish (2007) Enhanced permeability and retention of macromolecular drugs in solid tumors: A royal gate for targeted anticancer nanomedicines, *J Drug Target*. 15: 457-464.
- 3) S. Pasha, K. Gupta, (2010) Various drug delivery approaches to the central nervous system, *Expert Opin Drug Deliv*. 7: 113-135.
- 4) K. Kim, J.H. Kim, H. Park, Y.-S. Kim, K. Park, et al. (2010) Tumor-homing multifunctional nanoparticles for cancer theragnosis: Simultaneous diagnosis, drug delivery, and therapeutic monitoring, *J Control Release*. 146: 219-227.
- 5) M. Morille, C. Passirani, A. Vonarbourg, A. Clavreul, J.P. Benoit (2008) Progress in developing cationic vectors for non-viral systemic gene therapy against cancer, *Biomaterials*. 29: 3477-3496.
- 6) Y. Matsumura, H. Maeda (1986) A new concept for macromolecular therapeutics in cancer-chemotherapy - mechanism of tumorotropic accumulation of proteins and the antitumor agent smancs, *Cancer Res*. 46: 6387-6392.
- 7) Y. Kim, M.H. Pourgholami, D.L. Morris, M.H. Stenzel (2011) Triggering the fast release of drugs from crosslinked micelles in an acidic environment, *Journal of Materials Chemistry*, 21: 12777-12783.
- 8) P.D. Thornton, R.J. Mart, R.V. Ulijn (2007) Enzyme-responsive polymer hydrogel particles for controlled release, *Advanced Materials*, 19: 1252-1256.
- 9) M. Oishi, Y. Nagasaki (2010) Stimuli-responsive smart nanogels for cancer diagnostics and therapy, *Nanomedicine*. 5: 451-468.
- 10) Q. Gan, T. Wang, C. Cochrane, P. McCarron (2005) Modulation of surface charge, particle size and morphological properties of chitosan-TPP nanoparticles intended for gene delivery, *Colloids Surf B Biointerfaces*. 44: 65-73.
- 11) J. Kumirska, M. Czerwicka, Z. Kaczynski, A. Bychowska, K. Brzozowski, (2010) Application of Spectroscopic Methods for Structural Analysis of Chitin and Chitosan, *Mar Drugs*. 8: 1567-1636.
- 12) T.A. Sonia, C.P. Sharma (2011) Chitosan and Its Derivatives for Drug Delivery Perspective, *Chitosan for Biomaterials I*. 243: 23-53.
- 13) J.H. Park, Y.W. Cho, H. Chung, I.C. Kwon, S.Y. Jeong (2003) Synthesis and characterization of sugar-bearing chitosan derivatives: Aqueous solubility and biodegradability, *Biomacromolecules*, 4: 1087-1091.
- 14) K.H. Liu, S.Y. Chen, D.M. Liu, T.Y. Liu (2008) Self-assembled hollow nanocapsule from amphiphaticcarboxymethyl-hexanoyl chitosan as drug carrier, *Macromolecules*. 41: 6511-6516.
- 15) K. Kurita (2001) Controlled functionalization of the polysaccharide chitin, *Progress in Polymer Science*, 26: 1921-1971.
- 16) Sashiwa H, Kawasaki N, Nakayama A, Muraki E, Yamamoto N (2002) Chemical modification of chitosan. 13. Synthesis of organosoluble, palladium adsorbable, and biodegradable chitosan derivatives toward the chemical plating on plastics, *Biomacromolecules*. 3: 1120-1125.
- 17) Y.S. Wang, L.R. Liu, Q. Jiang, Q.Q. Zhang (2007) Self-aggregated nanoparticles of cholesterol-modified chitosan conjugate as a novel carrier of epirubicin, *European Polymer Journal*, 43: 43-51.
- 18) N. Bhattarai, J. Gunn, M. Zhang (2010) Chitosan-based hydrogels for controlled, localized drug delivery, *Adv Drug Deliv Rev*. 62: 83-99.
- 19) Y.I. Jeong, D.G. Kim, M.K. Jang, J.W. Nah (2008) Preparation and spectroscopic characterization of methoxy poly(ethylene glycol)-grafted water-soluble chitosan, *Carbohydr Res*. 343: 282-289.
- 20) T. Ouchi, H. Nishizawa, Y. Ohya (1998) Aggregation phenomenon of PEG-grafted chitosan in aqueous solution, *Polymer*, 39: 5171-5175.
- 21) Dong-Gon Kim, Young-Il Jeong, Jae-Woon Nah (2007) All-trans retinoic acid release from polyion-complex micelles of methoxy poly(ethylene glycol) grafted chitosan. *Journal of Applied Polymer Science*. 105: 3246-3254.
- 22) S.R. Mao, X.T. Shuai, F. Unger, M. Wittmar, X.L. Xie, et al. (2005) Synthesis, characterization and cytotoxicity of poly(ethylene glycol)-graft-trimethyl chitosan block copolymers, *Biomaterials*. 26: 6343-6356.
- 23) Y.Q. Hu, H.L. Jiang, C.N. Xu, Y.J. Wang, et al. (2005) Preparation and characterization of poly(ethylene glycol)-g-chitosan with water- and organosolubility, *Carbohydrate Polymers*. 61: 472-479.
- 24) H. Saito, X.D. Wu, J.M. Harris, A.S. Hoffman (1997) Graft copolymers of poly(ethylene glycol) (PEG) and chitosan, *Macromolecular Rapid Communications*. 18: 547-550.
- 25) J.H. Park, S.G. Kwon, J.O. Nam, R.W. Park, H. Chung, et al. (2004) Self-assembled nanoparticles based on glycol chitosan bearing 5 beta-cholanic acid for RGD peptide delivery, *J Control Release*. 95: 579-588.
- 26) Hwang HY, Kim IS, Kwon IC, Kim YH (2008) Tumor targetability and antitumor effect of docetaxel-loaded hydrophobically modified glycol chitosan nanoparticles, *J Control Release*. 128: 23-31.
- 27) Kim JH, Bae SM, Na MH, Shin H, Yang YJ (2012) Facilitated intracellular delivery of peptide-guided nanoparticles in tumor tissues. *J Control Release* 157: 493-499.
- 28) Kim JH, Kim YS, Park K, Lee S, Nam HY, et al. (2008) Antitumor efficacy of cisplatin-loaded glycol chitosan nanoparticles in tumor-bearing mice, *J Control Release*. 127: 41-49.
- 29) Kwangmeyung Kim, Jong-Ho Kim, Sungwon Kim, Hesson Chung, Kuiwon Choi, et al. (2005) Self-assembled nanoparticles of bile acid-modified glycol chitosans and their applications for cancer therapy, *Macromolecular Research*. 13: 167-175.
- 30) Sung Eun Kim, Ick Chan Kwon, Hae-Ryong Song, Kyeongsoon Park (2012) Insight of Key Factors Influencing Tumor Targeting Characteristics of Glycol Chitosan-Based Nanoparticles and In vivo Applications, *Macromolecular Research*. 20: 1109-1117.
- 31) Na JH, Koo H, Lee S, Min KH, Park K (2011) Real-time and non-invasive optical imaging of tumor-targeting glycol chitosan nanoparticles in various tumor models. *Biomaterials*. 32: 252-5261.
- 32) T. Luger, E.M. Kokoschka, P. Sagaster, M. Micksche (1979) Serum lysozyme levels in patients with solid tumors, *Oncology*. 36: 15-18.
- 33) A. Wohlkonig, J. Huet, Y. Looze, R. Wintjens (2010) Structural Relationships in the Lysozyme Superfamily: Significant Evidence for Glycoside Hydrolyase Signature Motifs, *Plos One*. 5: e15388.
- 34) S. Luo, E. Zhang, Y. Su, T. Cheng, C. Shi (2011) A review of NIR dyes in cancer targeting and imaging, *Biomaterials*. 32: 7127-7138.
- 35) D.K. Sen, G.S. Sarin (1986) Biological variations of lysozyme concentration in the tear fluids of healthy-persons. *Br J Ophthalmol*. 70: 246-248.

36) A.M. Cole, D.R. Thapa, V. Gabayan, H.I. Liao, L. Liu, et al. (2005) Decreased clearance of *Pseudomonas aeruginosa* from airways of mice deficient in lysozyme M, *J Leukoc Biol.* 78: 1081-1085.

37) Park K, Kim JH, Nam YS, Lee S, Nam HY. (2007) Effect of polymer molecular weight on the tumor targeting characteristics of self-assembled glycol chitosan nanoparticles, *J Control Release.* 122: 305-314.

38) Nam HY, Kwon SM, Chung H, Lee SY, Kwon SH, et al. (2009) Cellular uptake mechanism and intracellular fate of hydrophobically modified glycol chitosan nanoparticles, *Journal of Controlled Release*, 135: 259-267.

39) H. Onishi, Y. Machida (1999) Biodegradation and distribution of water-soluble chitosan in mice, *Biomaterials.* 20: 175-182.

Submit your manuscript to a JScholar journal and benefit from:

- ¶ Convenient online submission
- ¶ Rigorous peer review
- ¶ Immediate publication on acceptance
- ¶ Open access: articles freely available online
- ¶ High visibility within the field
- ¶ Better discount for your subsequent articles

Submit your manuscript at
<http://www.jscholaronline.org/submit-manuscript.php>